Biogeosciences Discussions

Biogeosciences Discussions is the access reviewed discussion forum of *Biogeosciences*

Nitrous oxide fluxes measured with quantum cascade laser system

W. Eugster et al.

Nitrous oxide net exchange in a beech dominated mixed forest in Switzerland measured with a quantum cascade laser spectrometer

W. Eugster[1], K. Zeyer[2], M. Zeeman[1], P. Michna[3], A. Zingg[4], N. Buchmann[1], and L. Emmenegger[2]

[1]Institute of Plant Sciences, ETH Zürich, 8092 Zürich, Switzerland
[2]Empa, Swiss Federal Laboratories for Materials Testing and Research, Überlandstrasse 129, 8600 Dübendorf, Switzerland
[3]Geographical Institute, University of Bern, 3012 Bern, Switzerland
[4]WSL, Swiss Federal Institute for Forest, Snow, and Landscape Research, 8903 Birmensdorf, Switzerland

Correspondence to: W. Eugster (werner.eugster@ipw.agrl.ethz.ch)

Title Page

Abstract	Introduction
Conclusions	References
Tables	Figures

◄◄	►►
◄	►
Back	Close

Full Screen / Esc

Printer-friendly Version

Interactive Discussion

EGU

Nitrous oxide fluxes measured with quantum cascade laser system

W. Eugster et al.

Abstract

Nitrous oxide fluxes were measured at the Lägeren CarboEurope IP flux site over the multi-species mixed forest dominated by European beech and Norway spruce. Measurements were carried out during a four-week period in October–November 2005 during leaf senescence. Fluxes were measured with a standard ultrasonic anemometer in combination with a quantum cascade laser absorption spectrometer that measured N_2O, CO_2, and H_2O mixing ratios simultaneously at 5 Hz time resolution. To distinguish insignificant fluxes from significant ones it is proposed to use a new approach based on the significance of the correlation coefficient between vertical wind speed and mixing ratio fluctuations. This procedure eliminated roughly 56% of our half-hourly fluxes. Based on the remaining, quality checked N_2O fluxes we quantified the mean efflux at $0.8 \pm 0.4 \, \mu\text{mol m}^{-2} \text{h}^{-1}$ (mean ± standard error). Most of the contribution to the N_2O flux occurred during a 6.5-h period starting 4.5 h before each precipitation event. No relation with precipitation amount could be found. Visibility data representing fog density and duration at the site indicate that wetting of the canopy may have as strong an effect on N_2O effluxes as does below-ground microbial activity. It is speculated that above-ground N_2O production from the senescing leaves at high moisture (fog, drizzle, onset of precipitation event) may be responsible for part of the measured flux. In comparison with the annual CO_2 budget of $-342 \, \text{g C m}^{-2} \text{yr}^{-1}$ it is estimated that concurrent N_2O fluxes offset at least 5% of the greenhouse forcing reduction via net CO_2 uptake.

1 Introduction

Water vapor, carbon dioxide, methane, and nitrous oxide are the four most important greenhouse gases in the atmosphere that strongly influence climate and thus also climate change. Whilst water vapor and carbon dioxide flux measurements are now standard within a more or less dense (depending on continent and remoteness) research network of flux stations known as FLUXNET (Baldocchi et al., 2001), in which the Eu-

ropean CarboEurope IP network is participating, only few sites are equipped with more difficult to perform methane or nitrous oxide (N_2O) flux measurements. N_2O has the greatest greenhouse forcing potential on a per-molecule basis (Houghton et al., 2001). Still, our knowledge of the individual sources and sinks is poor (Bouwman et al., 1995)

5   and does not adequately cover the large natural variability there is – or is expected – in N_2O fluxes from different ecosystems.

The general knowledge, summarized among others by Meixner and Eugster (1999) is that N_2O is produced mostly in an intermediate soil moisture range where soils are not too dry (which would allow better oxidation of nitrogen, and thus NO emissions) and

10 not too wet and anoxic (which would inhibit oxidation of nitrogen and thus rather lead to N_2 emissions). Since our CarboEurope IP forest site is located on a well-drained mountain slope in the Jura Mountains of Switzerland, it was not known whether N_2O effluxes from this site can safely be neglected in the overall greenhouse gas budget, or whether there is a need to include this component explicitly in our measurement

15 protocol. In this article we report eddy covariance flux measurements obtained during a field test of a newly developed and improved tunable quantum cascade laser absorption spectrometer (QCLAS) during a 4-week period in autumn 2005 at the Lägeren flux site in northern Switzerland. The questions we wanted to answer were: (1) Is this new instrument that does no longer require liquid nitrogen cooling ready for field deployment

20 at FLUXNET locations? (2) Does this technique provide all relevant information that is needed for a thorough assessment of its accuracy for eddy covariance flux measurements? And (3) what is the magnitude of N_2O fluxes from this forest ecosystem and how do they relate to wetting during precipitation events?

2   Site description

25 The Lägeren research site (CH-Lae in CarboEurope IP) is situated at 47°28′40.8″ N; 8°21′55.2″ E at 682 m a.s.l. (base of tower) on the south-facing slope of the Lägeren mountain (866 m a.s.l.), approximately 15 km northwest of Zurich, Switzerland. The

Nitrous oxide fluxes measured with quantum cascade laser system

W. Eugster et al.

Title Page

Abstract   Introduction

Conclusions   References

Tables   Figures

◄   ►►

◄   ►

Back   Close

Full Screen / Esc

Printer-friendly Version

Interactive Discussion

south slope of the Lägeren mountain marks the boundary of the Swiss Plateau, which is bordered by the Jura and the Alps. This site became a permanent station of the Swiss air quality monitoring network (NABEL) in 1986. First eddy covariance flux measurements were carried out during the winter season 2001/2002 to quantify fog water fluxes and the flux of dissolved inorganic ions therein (Burkard et al., 2003). Routine CO_2 and H_2O flux measurements as a contribution to the CarboEurope IP network started on 1 April 2004. Flux measurement instruments were installed on a horizontal boom extending from the top of a 49 m tower in south-western direction to yield a measurement height $Z = 59$ m above local ground.

The natural vegetation cover at the research site is a productive, managed beech forest. The western part is dominated by broad-leaved trees, mainly ash, sycamore and beech whereas in the eastern part beech and spruce are dominating (Table 1). The forest stand has a relatively high diversity concerning species, age, and diameter distribution. We counted 105 to 185 years for spruce and 52 to 155 years for beech. This structure is the result of a consequent intensive management by Swiss Selective Cutting and natural regeneration during the last decades after the transition to the so-called "permanent forest system". The mean tree height of the dominant trees was 30.6 m, the highest spruces reach 42.2 m. The aerodynamic displacement height d was estimated at 18 m, yielding an effective measurement height $z = Z - d$ of ≈30 m.

The pronounced linear topography of the Lägeren mountain ridge leads to a very nicely channeled atmospheric flow that is mostly along the slope with two distinct lobes of the flux footprint towards the West (primary maximum occurrence of wind direction) and the East (secondary maximum).

3 Methods

3.1 N$_2$O flux measurements with a Quantum Cascade Laser System

We used a QCLAS (Nelson et al., 2002) in combination with an ultrasonic anemometer (Gill Solent HS, sampling at 20 Hz) used as the standard instrument of the Lägeren Car-

5 boEurope IP flux site. In addition to the configuration described in Neftel et al. (2007), who used an earlier version of the same instrument, efforts were made to also quantify water vapor (H$_2$O) with the same laser that measures nitrous oxide (N$_2$O) and carbon dioxide (CO$_2$). The commercially available instrument (Aerodyne Research Inc., USA) was modified to obtain enhanced stability and precision under field conditions and to

10 simultaneously measure N$_2$O, CO$_2$ and H$_2$O with a single laser. Both the laser and the detector were thermoelectrically cooled, giving a cryogen-free instrument, which can run unattended for extended time periods. Accurate temperature control is necessary to tune the QC laser to the desired wavenumber (Fig. 1).

Samples were measured at 65 mbar in a 0.5 L astigmatic multipass absorption cell

15 with a path length of 56 m. At this pressure, the collisional broadening of the absorption lines is sufficiently small to allow the separation of the absorption lines and yield a well defined baseline (Fig. 1). The absorption spectra were fitted numerically based on a set of parameters including line positions, line strengths, broadening coefficients, and lower state energies taken from the HITRAN database (Rothman et al., 2005). Volume

20 mixing ratio values were calculated using the Beer-Lambert law.

The QC laser was driven with short ($\approx$10 ns) pulses in a 1% duty cycle at –31°C. The signal-to-noise ratio was enhanced by normalizing pulse-to-pulse intensity variations with temporal gating on a single detector. Data acquisition and analysis was done by TDLWintel, a commercially available software package (Nelson et al., 2004). Absorp-

25 tion spectra at 2241 cm^{-1} were recorded by sweeping the laser across the absorption features at a rate of about 5 kHz. Co-averaged spectra were quantified at 5 Hz. Background (N$_2$, 99.999%) and reference (pressurized air) spectra were measured every 30 min. This regular procedure is called autocalibration in the following text.

Spectroscopically determined mixing ratios of N_2O and CO_2 were calibrated taking into account the spectra of pressurized air that was traced to a CMDL standard (Climate Monitoring and Diagnostics Laboratory, NOAA, USA). For water, 10-min averages were compared to the values obtained using a Thygan VTP6 (Meteolabor, Switzerland) dewpoint mirror. The linear regression of the data from the full measurement campaign was forced through zero and gave a calibration factor of 1.09 (r^2=0.99). The precision for N_2O and CO_2 was determined every 30 min based on measurements of dry compressed air during 20 s. Typical values were 0.3 ppb root-mean-square error (at 1 Hz) for N_2O and 0.7 ppm root-mean-square error (at 1 Hz) for CO_2. For water, the corresponding value was about 50 ppm, determined from ambient air during periods with only small concentration changes.

The QCLAS was located in an air conditioned room, and samples were drawn at 149 L min^{-1} and –270 hPa through 55 m PVC tubing (inner diameter I.D. of 14 mm), the tip of which was attached close to the sonic anemometer. The intake was placed 0.2 m from the sonic anemometer's sensor head in the horizontal direction such that the air flow has no influence on the vertical wind speed measurements. A smaller Teflon hose (I.D.'4 mm) with a length of ≈ 3 meters was then connected to the instrument. This Teflon hose and the QCLAS sample cell were purged with a flow rate of 6 L min^{-1} using an oil-free vacuum pump (Varian Triscroll 300). The full sampling system was kept at turbulent flow conditions and had a time delay of ≈ 4 s with a response time (cell volume/flow) of 0.3 s. For the covariance computations the actual delay time for each 30-min averaging period was considered by searching for the maximum cross-correlation around this expected delay. A maximum delay of 5 s (25% longer than expected) was defined for this search.

3.2 N_2O flux calculations

The eddy covariance flux measurement method (e.g. Baldocchi, 2003, Eugster et al., 1997) is the standard method within CarboEuropeIP and well described by Aubinet et al. (2000) for the standard CO_2 and H_2O flux measurements that were also carried

Nitrous oxide fluxes measured with quantum cascade laser system

W. Eugster et al.

Title Page

Abstract | Introduction

Conclusions | References

Tables | Figures

|◄ | ►|

◄ | ►

Back | Close

Full Screen / Esc

Printer-friendly Version

Interactive Discussion

EGU

out at the Lägeren site using a Licor 7500 (Lincoln, Nebraska, USA) non-dispersive open-path infrared gas analyzer (IRGA). For the special purpose to add QCLAS flux measurements, we however had to modify our data acquisition and data processing method as described in the following.

The QCLAS data processing computer handed over the mixing ratio values of N_2O, CO_2, and H_2O at a rate of 5 Hz via a serial RS-232 data connection to the eddy covariance computer. In order not to disturb the covariance computations that are performed at regular 30-min intervals, these autocalibration procedures were scheduled to begin shortly before the half-hour time marks, and end shortly thereafter. Since the sonic anemometer and IRGA data arrived at 20 Hz, whereas the QCLAS data arrived at 5 Hz, the latter had to be replicated 4 times in the raw data set. When processing the raw data files with a further development of the software mentioned in Eugster et al. (1997) that has also undergone the CarboEurope IP software intercomparison (T. Foken, personal communication), we trimmed the 30-min periods to roughly 29 min periods separated by the missing data blocks during autocalibration. All other procedures, however, corresponded to the standard processing algorithm, except for (a) that a high-frequency damping loss correction as suggested by Eugster and Senn (1995) did not appear to be essential (see Sect. 4.2), and (b) that the correct application of the Webb et al. (1980) density flux correction had to be evaluated first (see Sect. 5.1).

3.3 Error assessment

A great proportion of our analyses presented in the following sections will assess uncertainties and errors (random and systematic) in our N_2O flux measurements. We will argue that since the eddy covariance approach is based on the general correlation equation we should be able to identify insignificant flux values via statistically insignificant correlation coefficients. The general correlation equation is (Wilks, 2006, p. 51)

$$r = \frac{\overline{w'c'}}{\sqrt{\overline{w'^2}} \cdot \sqrt{\overline{c'^2}}} \, , \tag{1}$$

Nitrous oxide fluxes measured with quantum cascade laser system

W. Eugster et al.

EGU

where r is Pearson's correlation coefficient, w is the measured wind speed component perpendicular to the dynamic streamlines (in $m\,s^{-1}$), and c is the concentration measurement. Overbars denote averages over time intervals, and primes denote short-term deviations thereof. The covariance $\overline{w'c'}$ is the turbulent flux of the entity, which depending on the type of measurement that c represents must be scaled accordingly to yield flux density values. For example, the CO_2 concentration delivered by the IRGA is in $mmol\,m^{-3}$, thus the CO_2 flux obtained from that instrument, directly yields $mmol\,m^{-2}\,s^{-1}$. In the case of the QCLAS that measures mixing ratio, the unit of c is ppb for N_2O, which corresponds to $nmol\,mol^{-1}$. The flux of N_2O measured with QCLAS it thus derived from the covariance (which yields $nmol\,mol^{-1}\,m\,s^{-1}$) multiplied by ρ_a/M_a, where ρ_a is the density of air (in $kg\,m^{-3}$), and M_a is the molar mass of air ($\approx 0.028965\,kg\,mol^{-1}$).

Signal-to-noise ratios (SNR) of the QCLAS data for a specific frequency f were defined as follows (see Eq. A2 in Eugster et al., 2003):

$$\mathrm{SNR}(f) = \sqrt{\frac{\overline{c(f)'^2}}{(\mathrm{RMS\ noise})^2} - 1} \, , \tag{2}$$

where RMS is the frequency-independent root-mean-square of the white noise level of the instrument (for determination of the white noise level see Sect. 4.1).

4   QCLAS instrument performance

4.1 N_2O Variance spectra

An example spectrum of measured N_2O variance is shown in Fig. 2a. Since we set the instrument to auto-calibrate itself every 30 min, the effective length of continuous data is $29'10''$ followed by a gap of $50''$. Thus, we cannot compute 1-h spectra as is generally done (cf. Kaimal et al., 1972) to see how spectral densities approach zero

with lower frequencies. Therefore, in our example we computed the spectral densities for half-hour periods, knowing that the densities at low frequencies are underestimated compared to those expected in uninterrupted hourly time series.

First of all, the spectrum in Fig. 2a shows the effect of oversampling. We collected data at 20 Hz, whereas we set the QCLAS to provide 5 Hz data. Although we could have set the QCLAS to output 20 Hz, this would have reduced the integration time per sample and thus increased the signal-to-noise ratio. Moreover, the volume of our sample cell, the tube length and flow rate suggest that our QCLAS can provide at most 2–3 Hz data. This estimate was determined experimentally, treating the sample cell as a mixed reactor and fitting rapid concentration changes according to

$$c_{N_2O}(t) = c_{N_2O}(0) \cdot \exp(-t/\tau) \ , \tag{3}$$

where t is the time in s and τ is the time constant. The time constant of the instrument alone is $\approx$0.3 s, and increases to $\approx$0.45 s for the full sampling setup. This corresponds to a low-pass filter with a cutoff frequency $f_c = 1/(2\pi\tau)$, which is 0.4 Hz for the full setup. Thus, a 5 Hz sampling rate (for which the Nyquist frequency is 2.5 Hz) seemed adequate. The noise of flux measurements depends on a complicated set of sensor properties such as the instrument's white noise, pink noise (e.g. drift), and response. These effects and interactions have already been discussed in more detail for a QCLAS by Saleska et al. (2006).

In Fig. 2a all information to the right of the broken vertical line – the Nyquist frequency that separates the resolved from the unresolved frequencies – is related to the oversampling of the QCLAS signal. The true noise level for N_2O is therefore not to be sought at the highest frequencies, but left of the Nyquist frequency. We chose a display in Fig. 2a where white noise is shown as horizontal lines. The transition from the inertial subrange slope indicated by the theoretical $f^{-5/3}$ decay of spectral density with increasing frequency towards the horizontal can nicely be seen. Thus, we defined the noise level of the QCLAS's N_2O signal to be the spectral density of the segment showing almost no dependency on frequency. This is a more conservative estimate

than just taking the spectral density at the Nyquist frequency.

With reference to this noise level we can see a clear QCLAS signal up to 1 Hz. As expected, the signal disappears at higher frequencies. Nevertheless, Fig. 2a shows that the overall performance of the QCLAS for eddy covariance flux measurements of

5 N_2O should be sufficient, at least for daytime conditions where the high frequencies are not contributing much to the total flux. Based on our definition of the instrument noise level, we can now compute the signal-to-noise ratios of the whole spectrum in Fig. 2a. For the energy containing range of the spectrum – the intermediate frequencies which are most relevant for turbulent mixing and exchange – we get very good ratios

10 of up to 20. The signal-to-noise ratio where the measured spectrum separates from the theoretical inertial subrange slope is found at a ratio of 3. The frequency where the measured spectrum drops below a ratio of 1 is indicated by the vertical arrow at $f = 0.19$ Hz.

Despite the very good signal-to-noise ratios for the energy containing range of the

15 N_2O spectra the instrument noise contributes almost 50% of the variance signal on the half-hourly averages displayed in Fig. 2a. This is much better seen when an area-preserving variant of the same information is given as in Fig. 2b, where the spectral densities were multiplied with f.

4.2 N_2O Flux cospectra

20 Figure 3 shows a rather good behavior in the high frequencies. Despite the fact that the QCLAS has a limited time response of 2–3 Hz, there is no need to apply any damping loss correction (Eugster and Senn, 1995). This is not unexpected since the most relevant information for eddy covariance flux measurements is found at much lower time scales than the response rate of the QCLAS. When comparing the cospectra with

25 idealized 1-h cospectral curves by Kaimal et al. (1972) (broken curve in Fig. 3), we see a very good agreement at frequencies >0.005 Hz. The difference at lower frequencies has two main reasons: (1) the autocalibration of the QCLAS at 30-min intervals results in shorter uninterrupted intervals of continuous data that in consequence lead to lower

Nitrous oxide fluxes measured with quantum cascade laser system

W. Eugster et al.

cospectral densities at low frequencies; and (2) the need for detrending the time series for the Fourier transformation (Panofsky and Dutton, 1984, Stull, 1988) further reduces the cospectral densities at lower frequencies. This may lead to conservative estimates of the N_2O flux estimates. Given the stability of the instruments we would opt for longer periods (1–2 h) between autocalibration in future studies.

5 Possible sources of error in N_2O flux measurements

There are many sources of errors that could potentially influence the eddy covariance measurements. It is unavoidable to screen out a certain fraction of data due to plausibility reasons. This is sometimes termed "quality control" and within CarboEurope IP it was agreed to use a common quality flag system that gives flag 0 for highest quality research grade data points, flag 1 for good quality data that are perfect for long-term budgeting of the fluxes, and flag 2 for all other data points, including missing values due to technical problems, power failures, and more. The concept goes back to that proposed by Foken and Wichura (1996). In practice, two checks are performed to yield the quality flag information: (1) a stationarity test, and (2) a test whether σ_w/u_* as a function of the stability parameter z/L (Monin and Obukhov, 1954) conforms with the empirical model suggested by Foken and Wichura (1996). For the first test (stationarity test) one compares the arithmetic mean of six 5-min flux averages with the 30-min covariance. If the deviation from an idealized 1:1 ratio – which could be expected if turbulence is not covering larger time scales than 5 min[1] – is <30%, <100%, or ≥100% then flags 0, 1, and 2, respectively, are given. This procedure is repeated for the second test, and the larger of the two flags is assigned to the respective data point. Still, some questions remain, as was demonstrated by Geissbühler et al. (2000): the uncertainty in this test itself lies mostly in the uncertainty to quantify z/L outside the neutral

---

[1]this assumption could be questioned; the theoretical ratio based on the Kaimal et al. (1972) cospectra for idealized conditions would actually be 0.92; see Eugster et al. (2003)

Title Page

Abstract | Introduction

Conclusions | References

Tables | Figures

◀ | ▶

◀ | ▶

Back | Close

Full Screen / Esc

Printer-friendly Version

Interactive Discussion

EGU

stability range, and a huge deviation of σ_w/u_* may just indicate that z/L was wrong.

For our purpose we assessed whether despite such criticism the current quality flagging system of CarboEurope IP could help to identify outliers and bad data points also in N_2O fluxes. But before being able to do so we need to identify questionable data points in a completely independent way. We did this by investigating which fluxes are significant and which ones may be random fluxes. This involves two steps: first we carefully discuss the issue of density flux corrections (Webb et al., 1980) and then we discuss the issue of statistical significance of N_2O fluxes, followed by the comparison with the CarboEurope IP flag system.

5.1 Density flux correction

Webb et al. (1980) presented the following equation for the density flux correction of eddy covariance flux measurements:

$$F = \underbrace{\overline{w'\rho_c'}}_{I} + \underbrace{\mu\left(\overline{\rho_c}/\overline{\rho_a}\right)\overline{w'\rho_v'}}_{II} + \underbrace{(1+\mu\sigma)\left(\overline{\rho_c}/\overline{T}\right)\overline{w'T'}}_{III} , \qquad (4)$$

where w is vertical wind speed in $m\,s^{-1}$, ρ_c, ρ_a, and ρ_v are the densities of gas c, air, and vapor, respectively, in $kg\,m^{-3}$, T is air temperature in K, and $\mu=m_a/m_v$ and $\sigma=\overline{\rho_v}/\overline{\rho_a}$. m_a and m_v are the molar masses ('weights') of dry air and water vapor, respectively, in the units $kg\,mol^{-1}$.

This equation has basically three additive terms: (I) the measured flux (or covariance), (II) a correction for concurrent moisture fluxes, and (III) a correction for concurrent sensible heat fluxes. As stated by Webb et al. (1980) terms II and III can be neglected in an instrument that measures the dry mole fraction. In the scientific community it is generally agreed that term III can be omitted in closed-path systems, while term II must be considered (as we did in our computations) unless the air is dried or moisture is measured and corrected for.

EGU

5.2 Significance of fluxes

N_2O flux measurements reported in the literature (see also Table 2) show large scatter and thus it is often difficult to distinguish true peak effluxes from randomly large fluxes. It is thus important to assess which flux values actually were significantly different from a random outcome. This is not necessarily identical to small fluxes, since significant fluxes result only from significant correlations when measured with the eddy covariance method. This shall be elaborated in more detail in this section. It becomes clear by studying Eq. (1) that it is meaningless to try to define a precise minimum detectable flux for eddy covariance systems as we would do for standard mean concentration measurements. The reason is that both components in the denominator of Eq. (1) are always greater than zero in a turbulent atmosphere, no matter whether there is a flux or not. This aspect will be illustrated in more detail in the following paragraphs.

We can test the significance of Pearson's correlation coefficient r using Student's t test,

$$t = r\sqrt{\frac{n-2}{1-r^2}} \, ,$$
(5)

(DMK/DPK, 1977, p. 93) where n is the number of samples per record (9000 at 5 Hz operation rate). By rearranging Eq. (5) we get the value for significant correlation,

$$r = \frac{t_p}{\sqrt{n-2+t_p^2}} \, ,$$
(6)

using the specified p value to determine t_p. Figure 4 clearly reveals the effect of insignificant correlation coefficients when compared against the values obtained with Eq. (6). We rejected all fluxes where either r was insignificant at $p \leq 0.0001$ (35.7% of records) or the momentum flux was not directed towards downwards (20.5%).

EGU

6 Results

The rigorous screening of insignificant N_2O fluxes left us with 44% accepted 30-min flux averages (Fig. 5). The rejected fluxes were rather randomly distributed over the whole time series, not indicative of any persistent systematic error that would leave gaps of several hours. Although there are no independent N_2O flux measurement available for validation, there is a possibility to compare CO_2 and H_2O fluxes from the QCLAS system against the standard IRGA flux measurements performed at 20 Hz.

In Fig. 6 the median diurnal cycles of the CO_2 and H_2O fluxes from both instruments are compared. Since the open-path IRGA system suffers reduced or bad data quality during rain and dense fog events, we had to further reduce the data set for such a comparison, screening out all periods where the IRGA reported above normal window dirtiness values (a house-keeping variable of the Licor 7500 indicating the current status of the open optical path). The median diurnal cycles agree quite well with a peak net CO_2 loss in the morning around 9 h (typical conditions with morning fog) and a minor peak uptake around 15 h when fog has normally cleared and evergreen conifers in the footprint of the flux measurements are still active even late in the growing season.

Similar to the findings for CO_2 flux the H_2O fluxes measured with QCLAS agree quite well with the IRGA system, although the variation around the median values is somewhat larger with the QCLAS. If this comparison reveals the system inherent properties of the QCLAS system also for N_2O fluxes then we can assume that the median order of magnitude of the N_2O flux in the diurnal cycle must be rather accurate.

6.1 The influence of rain and fog on N_2O fluxes

Since we do not yet have sufficient knowledge to develop an elaborate gap filling algorithm similar to the one used for energy and CO_2 flux series (see Falge et al., 2001), we chose a conservative approach and replaced all missing or rejected values by zero. This allowed us to compute a cumulative curve (Fig. 7), which reflects the influence of moisturizing events more clearly than with the 30-min fluxes alone.

EGU

Downward fluxes of N_2O were not objectively identified as erroneous or insignificant, but the cumulative curve in Fig. 7 clearly shows that there is a much stronger effect of effluxes from the ecosystem towards the atmosphere. Against our expectations that mostly soil processes and thus precipitation events would influence the overall magni-
5 tude of N_2O effluxes from this unfertilized forest, we did not find a strong correlation between precipitation amount and flux sum over an event. Some precipitation events, although with very little precipitation amounts, showed a very clear response in the N_2O flux time series, whereas especially the strong event on 22–23 October did not translate to similarly strong N_2O fluxes.
10 During the same time another research project had a field test running with a PWD-11 visibility sensor from Vaisala OY (Finland) to quantify fog (see Nylander et al., 1997 for technical details). Because the sensor was unmounted in the end of October, visibility information is only available until 25 October. When we compared N_2O fluxes also with fog densities (represented by horizontal visibilities, see Fig. 7, top panel), we
15 found strong indication that especially between 15 and 22 October, when only traces of precipitation were measured, the N_2O fluxes tended to respond to dense fog if it persisted over several hours (Fig. 8). From earlier measurements carried out by Burkard et al. (2003) and Bützberger (2002) we know that dense and persistant fog at the Lägeren site does not normally produce significant throughfall, but it wettens the forest
20 canopy. This, however does not chang soil moisture since no throughfall occurs (data not shown). Thus, a response seen in N_2O fluxes cannot exclusively be related to changes in soil moisture conditions as one would expect. This hypothesis also holds for precipitation events as can be seen in Fig. 9. Cumulative N_2O fluxes during a 24-h period starting 12 h before the first measured rain until 12 h thereafter were normalized
25 to have the zero crossing at the end of the 10-min period where rain was measured (that is, more than 0.1 mm of precipitation accumulated in the precipitation gauge). If N_2O fluxes did only respond to soil wetting via distinct precipitation events, then we would have expected that an increase in N_2O fluxes is only observed starting with that event, but not before it. In our analyses in Fig. 9, the general picture evolving from all 10

precipitation events is that an increase in N_2O fluxes starts around 4.5 h prior to the first measurable precipitation and ends already roughly 2 h afterwards. During this period, on average $18.3\pm8.4\,\mu mol\,m^{-2}\,h^{-1}$ were lost from the forest ecosystem (Table 2). This compares with an average $0.8\pm0.4\,\mu mol\,m^{-2}\,h^{-1}$ efflux observed over the full period of
5 23.25 days shown in Fig. 7, more than an order of magnitude in difference.

From this we can speculate that the wetting of the vegetation canopy, either by fog, by increased atmospheric moisture before precipitation sets in, or by the drizzle or rain that does not produce ≥0.1 mm of precipitation but which is not uncommon before measurable precipitation occurs, is much more important for driving N_2O effluxes than
10 precipitation amount. This implies that it is unlikely that soil microbial activity are the sole source of N_2O because fog deposition and drizzle before rain rather moisten the canopy and not the soil. Thus, the degradation of senescent leaves of deciduous trees at that time of year may be the most important source of N_2O.

7 Discussion

15 Our results suggest a clear increase in net ecosystem N_2O effluxes during a relatively short period around the beginning of a precipitation event only, but no clear relationship with total rainfall. Therefore, we scaled up our measurements to a conservative annual sum using our best N_2O loss estimate of $120\,\mu mol\,m^{-2}$ per precipitation event (6.5 h at $18.3\,\mu mol\,m^{-2}\,h^{-1}$; see Table 2) in the following way. In order to take account of
20 the fact that short events in a row do not have the same effect on N_2O fluxes as do events after a clear dry period (Fig. 7), we determined the average duration of rain-free periods in 2005 and defined the number of relevant precipitation events in one year as 365 days divided by this number. On average, periods between measurable rainfall recorded at 10-min resolution had a duration of 6.8 days, yielding 54 events per
25 year. From this the estimated annual sum of net N_2O losses is $6.5\pm3.0\,mmol\,m^{-2}\,yr^{-1}$ ($0.7\pm0.3\,\mu mol\,m^{-2}\,h^{-1}$ in Table 2). We consider this a conservative estimates since we do not account for N_2O fluxes between rain events which most likely will increase our

Nitrous oxide fluxes measured with quantum cascade laser system

W. Eugster et al.

Title Page

Abstract | Introduction

Conclusions | References

Tables | Figures

◀ | ▶

◀ | ▶

Back | Close

Full Screen / Esc

Printer-friendly Version

Interactive Discussion

estimate. On the other hand side, Kitzler et al. (2006) report significant uptake during winter when there is snow, a factor that might also be relevant at our site and which would act in the opposite direction.

Assuming a greenhouse warming potential of 226 CO_2 equivalents for each N_2O molecule suggests an N_2O contribution of $1.5\,\mathrm{mol\,m^{-2}\,yr^{-1}}$ CO_2 equivalents or $18\,\mathrm{g\,C\,m^{-2}\,yr^{-1}}$. This contribution is offsetting $\approx 5\%$ of the annual CO_2 uptake of $-342\,\mathrm{g\,C\,m^{-2}\,yr^{-1}}$ determined from November 2004 to October 2005 using an u_* threshold of $0.95\,\mathrm{m\,s^{-1}}$ to correct for underestimation of nocturnal CO_2 effluxes as measured with our eddy covariance system.

There are only very few ecosystem-scale eddy covariance N_2O flux measurements over forest available (Table 2) with which our fluxes could be compared. The measurements carried out in an old beech forest in Denmark (Pihlatie et al., 2005) shows trunk-space eddy covariance flux measurements during spring. The duration of their measurements is similar to ours (5 vs. 4 weeks) and their average fluxes were in the same order of magnitude as ours. The factor two difference may be a result of above-canopy (our study) vs. below-canopy measurements, different soil properties and microbial activities (autumn has warmer soils than spring), or phenology as we noted above. The Pihlatie et al. (2005) study also shows a very convincing comparison of eddy covariance flux measurements with automatic and manual chamber measurements (Table 2. Their chamber fluxes are roughly a factor two larger than their eddy covariance fluxes. Kitzler et al. (2006) measured bi-weekly during two years with manual chambers in a similar forest with comparable nitrogen deposition rates (see Burkard et al., 2003 for conditions at our site) and yielded mean N_2O fluxes of $0.31\pm0.02\,\mathrm{\mu mol\,m^{-2}\,h^{-1}}$. Although vegetation, soil type and calcareous ground are very comparable to the Lägeren site, their measurements were at a higher elevation where trees are less tall and annual temperature is $1.7°C$ colder (6.5 vs. $8.2°C$) which may already be responsible for the differences in fluxes. Differences are larger in the comparison with the fluxes measured over boreal aspen forest (Simpson et al., 1997) which shows fluxes that are almost an order of magnitude smaller. This might again be an indication of the colder climate

Nitrous oxide fluxes measured with quantum cascade laser system

W. Eugster et al.

leading to lower N_2O fluxes.

In comparison with agricultural ecosystems (Table 2) the N_2O fluxes from our mixed deciduous forest during rain events are very similar to those from agricultural fields after fertilization. This was not expected and should receive more attention in future studies. Furthermore, there is a need to increase our understanding of N_2O uptake reported in many studies (Pihlatie et al., 2005; Leahy and Kiely, 2006; Kitzler et al., 2006; Neftel et al., 2007) which is also evident in our data (Table 2) in order not to overestimate the greenhouse forcing effect of N_2O fluxes from natural ecosystems.

8 Conclusions

Net N_2O efflux from a deciduous tree dominated mixed forest in Switzerland averaged $0.8 \pm 0.4\,\mu\text{mol}\,\text{m}^{-2}\,\text{h}^{-1}$. Although these values are in the range reported by others (Table 2), these fluxes are relatively small and difficult to measure with currently available technology. Thus, a rigorous screening of data obtained from our Quantum Cascade Laser Absorption Spectrometer was necessary. Since we used the eddy covariance method for flux measurements we argued that the significance-of-correlation approach that uses the maximum cross-correlation value between vertical wind speed component and concentration fluctuations is a good statistical approach to separate significant fluxes from insignificant fluxes.

To the best of our knowledge this was the first attempt to simultaneously determine N_2O, CO_2 and H_2O with a single QC laser. The agreement of H_2O concentrations and fluxes with a standard Licor 7500 open-path IRGA was very encouraging and supports the idea that future developments should include this additional H_2O measurement to compute true dry-mole fractions for N_2O that would eliminate the need to apply a Webb et al. (1980) moisture density flux correction. We however showed that this correction is only small and it is not expected to have a large influence on our interpretation of eddy covariance N_2O fluxes measured with QCLAS. Unexpected was the relatively bad agreement between CO_2 flux measurements obtained from the QCLAS although CO_2

Nitrous oxide fluxes measured with quantum cascade laser system

W. Eugster et al.

concentrations (not shown) were in very good agreement with the IRGA. Thus, with the current instrument it would not be possible to replace a traditional IRGA if also CO_2 fluxes are of interest.

We estimated that the N_2O fluxes offset approximately 5% of the annual net CO_2 uptake of $-342\,g\,C\,m^{-2}\,yr^{-1}$ of this forest ecosystem in terms of carbon dioxide equivalents. A more detailed assessment of the forestry management practices, especially the estimation of wood harvests and the C export via this pathway will increase the relative importance of N_2O fluxes in future assessments and should be continued beyond the time frame of the CarboEuropeIP project. Besides the expected outcome that N_2O fluxes respond to precipitation events we hypothesized that canopy wetting by fog and drizzle must also be a relevant, yet unexplored process leading to N_2O emissions from above-ground biomass, probably from senescent leaves. In future studies it would be desirable to cover longer periods and assess the effect of phenology in deciduous tree dominated forests in more detail.

References

Aubinet, M., Grelle, A., Ibrom, A., Rannik, Ü., Moncrieff, J., Foken, T., Kowalski, A. S., Martin, P. H., Berbigier, P., Bernhofer, C., Clement, R., Elbers, J., Granier, A., Grunwald, T., Morgenstern, K., Pilegaard, K., Rebmann, C., Snijders, W., Valentini, R., and Vesala, T.: Estimates of the annual net carbon and water exchange of forests: The EUROFLUX methodology, Adv. Ecol. Res., 30, 113–175, 2000. 1172

Baldocchi, D., Falge, E., Gu, L., Olson, R., Hollinger, D., Running, S., Anthoni, P., Bernhofer, C., Davis, K., Evans, R., Fuentes, J., Goldstein, A., Katul, G., Law, B., Lee, X., Malhi, Y., Meyers, T., Munger, W., Oechel, W., Paw U, K. T., Pilegaard, K., Schmid, H. P., Valentini, R., Verma, S., Vesala, T., Wilson, K., and Wofsy, S.: FLUXNET: A New Tool to Study the Temporal

BGD

4, 1167–1200, 2007

Nitrous oxide fluxes measured with quantum cascade laser system

W. Eugster et al.

Title Page

Abstract	Introduction
Conclusions	References
Tables	Figures

Back | Close

Full Screen / Esc

Printer-friendly Version

Interactive Discussion

EGU

and Spatial Variability of Ecosystem-Scale Carbon Dioxide, Water Vapor, and Energy Flux Densities, Bull. Am. Meteorol. Soc., 82, 2415–2434, 2001. 1168

Baldocchi, D. D.: Assessing the Eddy Covariance Technique for Evaluating Carbon Dioxide Exchange Rates of Ecosystems: Past, Present and Future, Global Change Biol., 9, 479–492, 2003. 1172

Bouwman, A. F., van der Hoek, K. W., and Olivier, J. G. J.: Uncertainties in the Global Source Distribution of Nitrous Oxide, J. Geophys. Res., 100, 2785–2800, 1995. 1169

Burkard, R., Bützberger, P., and Eugster, W.: Vertical fogwater flux measurements above an elevated forest canopy at the Lägeren research site, Switzerland, Atmos. Environ., 37, 2979–2990, doi:10.1016/S1352-2310(03)00254-1, 2003. 1170, 1181, 1183

Bützberger, P.: Processes and contributions of occult and wet nutrient deposition to an elevated mixed forest in Switzerland, Master's thesis, Institute of Geography, University of Bern, 2002. 1181

DMK/DPK, ed.: Formeln und Tafeln: Mathematik – Statistik – Physik, Orell Füssli Verlag, 232 pp. ISBN 3-280-00905-7, 1977. 1179

Edwards, G. C., Thurtell, G. W., Kidd, G. E., Dias, G. M., and Wagner-Riddle, C.: A diode laser based gas monitor suitable for measurement of trace gas exchange using micrometeorological techniques, Agric. Forest Meteorol., 115, 71–89, 2003. 1191

Eugster, W. and Senn, W.: A Cospectral Correction Model for Measurement of Turbulent NO_2 Flux, Boundary-Layer Meteorol., 74, 321–340, 1995. 1173, 1176, 1194

Eugster, W., McFadden, J. P., and Chapin, III, F. S.: A Comparative Approach to Regional Variation in Surface Fluxes Using Mobile Eddy Correlation Towers, Boundary-Layer Meteorol., 85, 293–307, 1997. 1172, 1173

Eugster, W., Kling, G., Jonas, T., McFadden, J. P., Wüest, A., MacIntyre, S., and Chapin, III, F. S.: CO_2 Exchange Between Air and Water in an Arctic Alaskan and Midlatitude Swiss Lake: Importance of Convective Mixing, J. Geophys. Res., 108, 4362–4380, doi:10.1029/2002JD002653, 2003. 1174, 1177

Falge, E., Baldocchi, D. D., Iolson, R., Anthoni, P., Aubinet, M., Bernhofer, C., Burba, G., Ceulemans, R., Clement, R., Dolman, H., Granier, A., Gross, P., Grünwald, P., Hollinger, D., Jensen, J., Katul, G., Keronen, P., Kowalski, A., Ta Lai, C., Law, B., Meyers, T., Moncrieff, J., Moors, E., Munger, J. W., Pilegaard, K., Rannik, Ü., Rebmann, C., Suyker, A., Tenhunen, J. D., Tu, K. P., Verma, S., Vesala, T., Wilson, K., and Wofsy, S.: Gap filling strategies for long term energy flux data sets, Agric. Forest Meteorol., 107, 71–77, 2001. 1180

Nitrous oxide fluxes measured with quantum cascade laser system

W. Eugster et al.

Title Page

Abstract	Introduction
Conclusions	References
Tables	Figures

◄ | ►►

◄ | ►

Back | Close

Full Screen / Esc

Printer-friendly Version

Interactive Discussion

EGU

Foken, T. and Wichura, B.: Tools for Quality Assessment of Surface-Based Flux Measurements, Agric. Forest Meteorol., 78, 83–105, 1996. 1177

Geissbühler, P., Siegwolf, R., and Eugster, W.: Eddy Covariance Measurements on Mountain Slopes: The Advantage of Surface-normal Sensor Orientation Over a Vertical Set-up, Boundary-Layer Meteorol., 96, 371–392, 2000. 1177

Glickman, T. S., ed.: Glossary of Meteorology, American Meteorological Society, Boston, MA, 2 edn., 2000. 1198

Houghton, J. T., Ding, Y., Griggs, D. J., Noguer, M., van der Linden, P. J., Dai, X., Maskell, K., and Johnson, C. A., eds.: Climate Change 2001: The Scientific Basis. Contribution of Working Group I to the Third Assessment Report of the Intergovernmental Panel on Climate Change, Cambridge University Press, Cambridge (UK), New York, 881 pp., 2001. 1169

Kaimal, J. C., Wyngaard, J. C., Izumi, Y., and Coté, O. R.: Spectral Characteristics of Surface-Layer Turbulence, Quart. J. Roy. Meteorol. Soc., 98, 563–589, 1972. 1174, 1176, 1177, 1194

Kitzler, B., Zechmeister-Boltenstern, S., Holtermann, C., Skiba, U., and Butterbach-Bahl, K.: Controls over N_2O, NO_x and CO_2 fluxes in a calcareous mountain forest soil, Biogeosciences, 3, 383–395, 2006,
http://www.biogeosciences.net/3/383/2006/. 1183, 1184, 1191

Laville, P., Jambert, C., Cellier, P., and Delmas, R.: Nitrous oxide fluxes from a fertilised maize crop using micrometeorological and chamber methods, Agric. Forest Meteorol., 96, 19–38, 1999. 1191

Leahy, P. and Kiely, G.: Micrometeorological observations of nitrous oxide uptake by fertilized grassland, in: Open Science Conference on The GHG Cycle in the Northern Hemisphere, NI4, p. 148, CarboEurope, Sissi-Lassithi, Crete, 2006. 1184

Meixner, F. X. and Eugster, W.: Effects of Landscape Pattern and Topography on Emissions and Transport, pp. 147–175, Report of the Dahlem Workshop held in Berlin, January 18–23, 1998, John Wiley & Sons Ltd., Chichester, 367 p., 1999. 1169

Monin, A. S. and Obukhov, A. M.: Osnovnye zakonomernosti turbulentnogo peremešivaniâ v prizemnom sloe atmosfery, Trudy geofiz. inst. Akad. Nauk SSSR, 24, 163–187 (in Russian), 1954. 1177

Neftel, A., Flechard, C., Amman, C., Conen, F., Emmenegger, L., and Zeyer, K.: Experimental assessment of N_2O background fluxes in grassland systems, Tellus, p. revised, 2007. 1171, 1184, 1191

Nelson, D. D., Shorter, J. H., McManus, J. B., and Zahniser, M. S.: Sub-part-per-billion detection of nitric oxide in air using a thermoelectrically cooled mid-infrared quantum cascade laser spectrometer, Applied Physics B-Lasers and Optics, 75, 343–350, 2002. 1171

Nelson, D. D., McManus, B., Urbanski, S., Herndon, S., and Zahniser, M. S.: High precision measurements of atmospheric nitrous oxide and methane using thermoelectrically cooled mid-infrared quantum cascade lasers and detectors, Spectrochimica Acta Part a-Molecular and Biomolecular Spectroscopy, 60, 3325–3335, 2004. 1171

Nylander, P., Ström, L., Torikka, S., Sairanen, M., and Utela, P.: Present Weather Detector PWD11 - User's Guide, Vaisala, Helsinki, 82 pp., 1997. 1181

Panofsky, H. A. and Dutton, J. A.: Atmospheric Turbulence, John Wiley & Sons, New York, 397 pp., 1984. 1177

Pattey, E., Strachan, I. B., Desjardins, R. L., Edwards, G. C., Dow, D., and MacPherson, J. I.: Application of a tunable diode laser to the measurement of CH4 and N2O fluxes from field to landscape scale using several micrometeorological techniques, Agricultural And Forest Meteorology, 136, 222–236, 2006. 1191

Pihlatie, M., Rinne, J., Ambus, P., Pilegaard, K., Dorsey, J. R., Rannik, U., Markkanen, T., Launiainen, S., and Vesala, T.: Nitrous oxide emissions from a beech forest floor measured by eddy covariance and soil enclosure techniques, Biogeosciences, 2, 377–387, 2005, http://www.biogeosciences.net/2/377/2005/. 1183, 1184, 1191

Rothman, L. S., Jacquemart, D., Barbe, A., Benner, D. C., Birk, M., Brown, L. R., Carleer, M. R., Chackerian, C., Chance, K., Coudert, L. H., Dana, V., Devi, V. M., Flaud, J. M., Gamasche, R. R., Goldman, A., Hartmann, J. M., Jucks, K. W., Maki, A. G., Mandin, J. Y., Massie, S. T., Orphal, J., Perrin, A., Rinsland, C. P., Smith, M. A. H., Tennyson, J., Tolchenov, R. N., Toth, R. A., Vander Auwera, J., Varanasi, P., and Wagner, G.: The HITRAN 2004 molecular spectroscopic database, Journal of Quantitative Spectroscopy and Radiative Transfer, 96, 139–204, 2005. 1171

Saleska, S. R., Shorter, J. H., Herndon, S., Jimenez, R., McManaus, J. B., Munger, W., Nelson, D. D., and Zahniser, M.: What are the instrumentation requirements for measuring the isotopic composition of net ecosystem exchange of CO2 using eddy covariance methods?, Isotopes in Environmental and Health Studies, 42(2), 115–133, 2006. 1175

Scanlon, T. M. and Kiely, G.: Ecosystem-scale Measurements of Nitrous Oxide Fluxes for an Intensely Grazed, Fertilized Grassland, Geophys. Res. Lett., 30, 1852–1855, doi:10.1029/2003GL017454, 2003. 1191

Nitrous oxide fluxes measured with quantum cascade laser system

W. Eugster et al.

Simpson, I. J., Edwards, G. C., Thurtell, G. W., den Hartog, G., Neumann, H. H., and Staebler, R. M.: Micrometeorological measurements of methane and nitrous oxide exchange above a boreal forest, J. Geophys. Res., 102, 29 331–29 341, 1997. 1183, 1191

Stull, R. B.: An Introduction to Boundary Layer Meteorology, Kluwer, Dordrecht, 666 pp., 1988. 1177

Webb, E. K., Pearman, G. I., and Leuning, R.: Correction of flux measurements for density effects due to heat and water vapour transfer, Quart. J. R. Met. Soc., 106, 85–100, 1980. 1173, 1178, 1184, 1196

Wienhold, F. G., Frahm, H., and Harris, G. W.: Measurements of N_2O fluxes from fertilized grassland using a fast response tunable diode laser spectrometer, J. Geophys. Res., 99, 16 557–16 567, 1994. 1191

Wienhold, F. G., Welling, M., and Harris, G. W.: Micrometeorological Measurement and Source Region Analysis of Nitrous Oxide Fluxes from an Agricultural Soil, Atmos. Environ., 29, 2219–2227, 1995. 1191

Wilks, D. S.: Statistical Methods in the Atmospheric Sciences, vol. 91 of International Geophysical Series, Academic Press, San Diego, 2 edn., 627 p., 2006. 1173

Nitrous oxide fluxes measured with quantum cascade laser system

W. Eugster et al.

Title Page

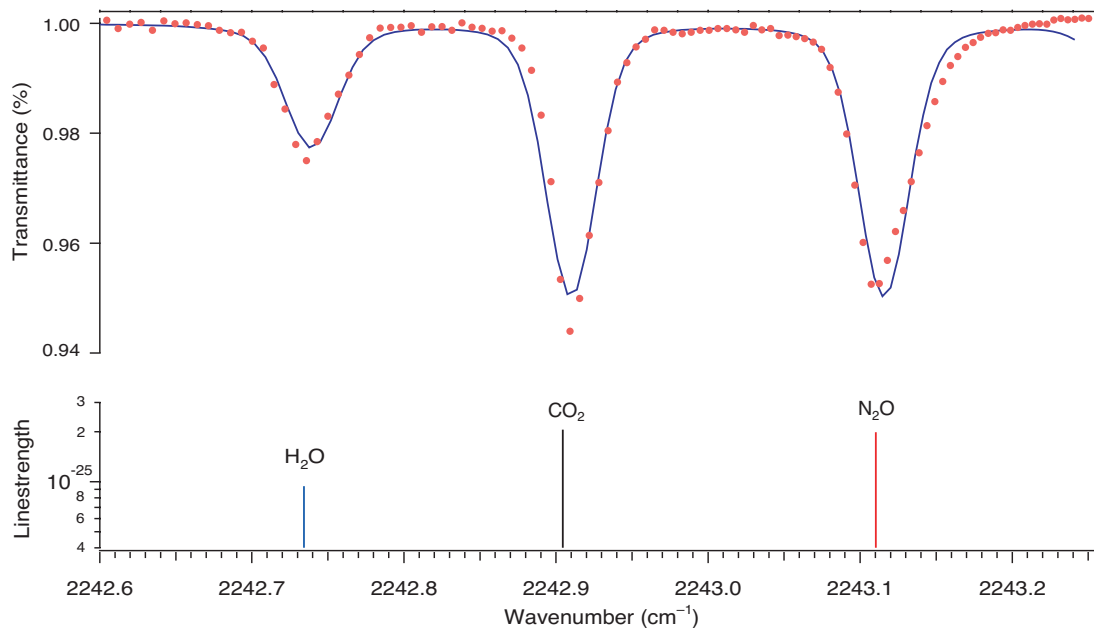| Abstract | Introduction |
| Conclusions | References |
| Tables | Figures |

◄ | ►

◄ | ►

Back | Close

Full Screen / Esc

Printer-friendly Version

Interactive Discussion

EGU

Table 1. Tree canopy species composition and above-ground stem wood volumes in the western, the eastern, as well as the total flux footprint area of the Lägeren tower. Data were collected during the winter season 2005/2006.

Tree species	English name	West	East $m^3 ha^{-1}$	Mean
Fagus sylvatica	European beech	59	213	136
Picea abies	Norway spruce	49	174	112
Fraxinus excelsior	Ash	146	38	92
Acer pseudoplatanus	Sycamore	123	35	79
Abies alba	Silver fir	24	95	60
Tilia cordata	Linden	36	2	19
Quercus robur	Oak	0	36	18
Ulmus glabra	Elm	28	8	18
Pinus sylvestris	Scots pine	0	10	5
Prunus avium	Cherry tree	8	0	4
Carpinus betulus	European hornbeam	2	1	2
Betula pendula	Birch	0	1	1
Sorbus aucuparia	Rowan	0	1	1
Total volume (stem wood >7 cm diameter)		475	613	544
Coniferous trees		73	279	176
Deciduous trees		402	334	368
Percentage of deciduous trees		84.6%	54.5%	67.6%

Table 2. Comparison of eddy covariance N_2O flux measurements over forests with selected results from agricultural ecosystems.

Ecosystem & Locality Measure	Chamber Flux μmol m^{-2} h^{-1}	Eddy Flux μmol m^{-2} h^{-1}	Reference
Forest ecosystems			
Mixed beech & spruce forest; Switzerland, Lägeren			This study
Autumn, 4 weeks		0.8±0.4	
Rain events (N_2O losses only during ≤6.5 h)		18.3±8.4	
Annual estimate		0.7±0.3	
Interquartile range		−2.7...5.0	
Absolute min...max		−22...83	
Old beech; Denmark, Lille Bøgeskov[a]			Pihlatie et al. (2005)
Spring mean, 5 weeks	0.7±0.1 / 1.1±0.8	0.4±0.1	
Median	0.7 / 0.6	0.3	
Range	0.01...2.1/−0.3...6.7	−0.1...1.5	
Boreal aspen forest; Canada, Saskatchewan			Simpson et al. (1997)
Full period, summer, 5 months		0.11±0.06	
Range		0.16...0.20	
Spruce-fir-beech forest; Austria, Tyrol			Kitzler et al. (2006)
Two years, bi-weekly sampling	0.31±0.02		
Agricultural ecosystems			
Agriculture, fertilized; UK, Scotland, Stirling			Wienhold et al. (1994)
Range, April		9.8...29	
Harvested wheat field; Denmark, NW Sealand, August			Wienhold et al. (1995)
Range		3.3...9.8	
Manured plot; Canada Ontario			Edwards et al. (2003)
Average		low fluxes	
Peak after 120 mm rain		117	
Corn field after fertilization; Canada, Ottawa			Pattey et al. (2006)
Baseline period		<2.9	
After fertilization, 67 mm rain		8.2...14.7	
Peak emissions		45	
40 days after fertilization		7...15	
Final week		2.9...6.6	
Maize fields, irrigated and fertilized; France, Landes de Gascogne			Laville et al. (1999)
Range	6.4...71	5.1...103	
Grassland, intensively grazed and fertilized; Ireland, Cork			Scanlon and Kiely (2003)
Background below		< 7.7	
Mean over 8 months		≈ 5.6	
Peak emissions (3 events)		≈130...250	
Grassland, fertilized; Switzerland, Oensingen			Neftel et al. (2007)
Background range	<8.2	−3.3...4.1	
Uptake events	≥−7.4		
Intercomparison, August	−0.5±0.2	1.1±0.3	

[a] Eddy covariance flux measurements were performed in the trunk space of the canopy, not above the canopy; both automatic and manual chamber measurements are given, separated by a slash (/).

Fig. 1. Experimental (dots) and simulated (line) transmission spectrum of H_2O, CO_2 and N_2O. The corresponding line strength (molecule^{-1} cm^{-1}) are given for typical ambient concentrations.
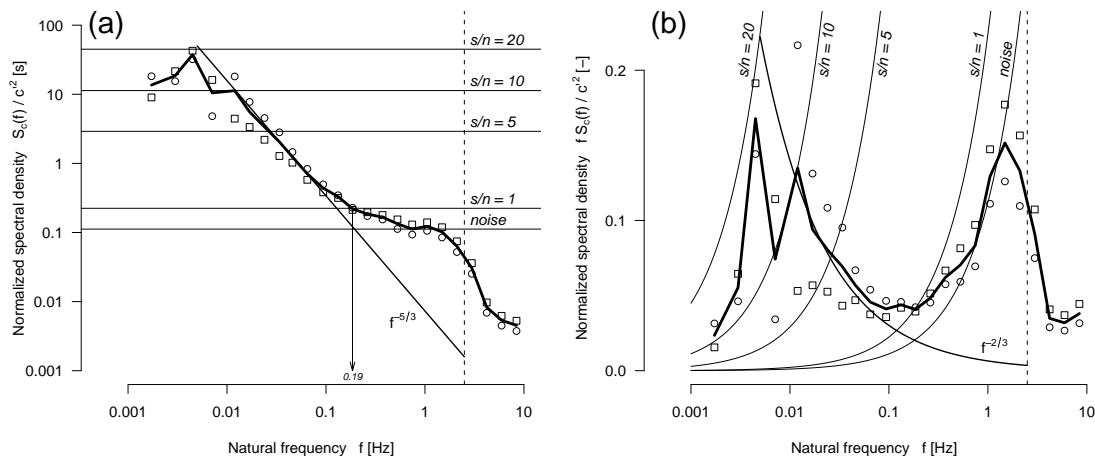
Fig. 2. Example spectra of N_2O variance from 30 October 2006, 11:00–12:00 CET, **(a)** in log–log and **(b)** in log–linear display where spectral densities $S_c(f)$ were multiplied with f to preserve areas below the spectral curve (in bold). Symbols show bandwidth averaged spectral densities of the first and second half hour, respectively, with the bold line the average of both. The expected inertial subrange slope is indicated by the $f^{-5/3}$ line in (a) and the $f^{-2/3}$ in (b), respectively. The vertical broken line shows the Nyquist frequency of the QCLAS data acquisition (2.5 Hz). Thin horizontal (a) or curved lines (b) give the noise level of the instrument and the corresponding levels for signal-to-noise ratios of 1, 5, 10, and 20, respectively. The arrow shows the frequency where the QCLAS signal-to-noise ratio is 1. Mean horizontal wind speed during the period was $0.78\,\mathrm{m\,s^{-1}}$. See text for interpretation.
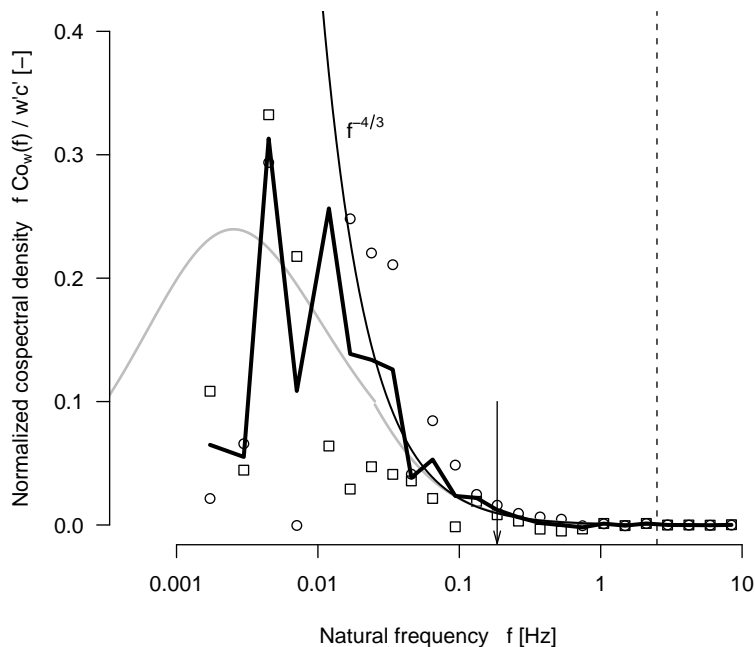
Fig. 3. Cospectra of N_2O fluxes from 30.10.2006, 11:00–12:00 CET. Symbols show bandwidth averaged cospectral densities of the first and second half hour, respectively, with the bold line the average of both. The gray line shows the idealized undamped cospectrum according to Kaimal et al. (1972) for one-hour runs (two times the length of the runs used here), and thin $f^{-4/3}$ curve shows the expected curvature of the inertial subrange. The vertical broken line shows the Nyquist frequency of the QCLAS data acquisition (2.5 Hz). Despite the QCLAS's limited frequency resolution, there is no strong sign of high-frequency damping losses that would require to use the Eugster and Senn (1995) correction model. The arrow shows the frequency where the QCLAS signal-to-noise ratio is 1.
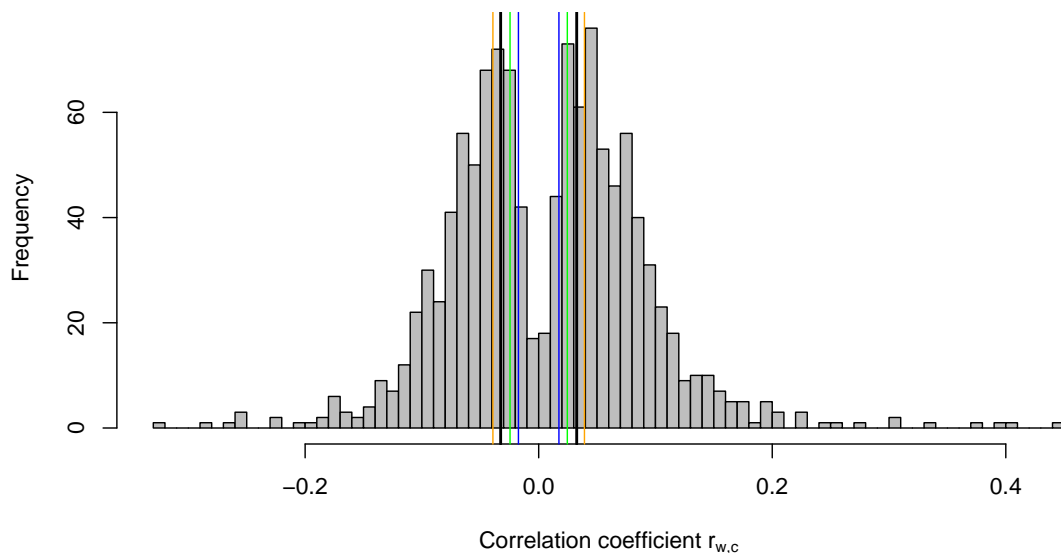
Fig. 4. Histogram of correlation coefficients according to Eq. (1) for QCLAS N_2O flux measurements. The colored vertical lines show the significance thresholds for $p = 0.05$, 0.01, 0.001, and 0.0001, respectively. For clarity, $p = 0.001$ is drawn with thicker lines. Insignificant fluxes result from insignificant correlations between the the two groups of lines.
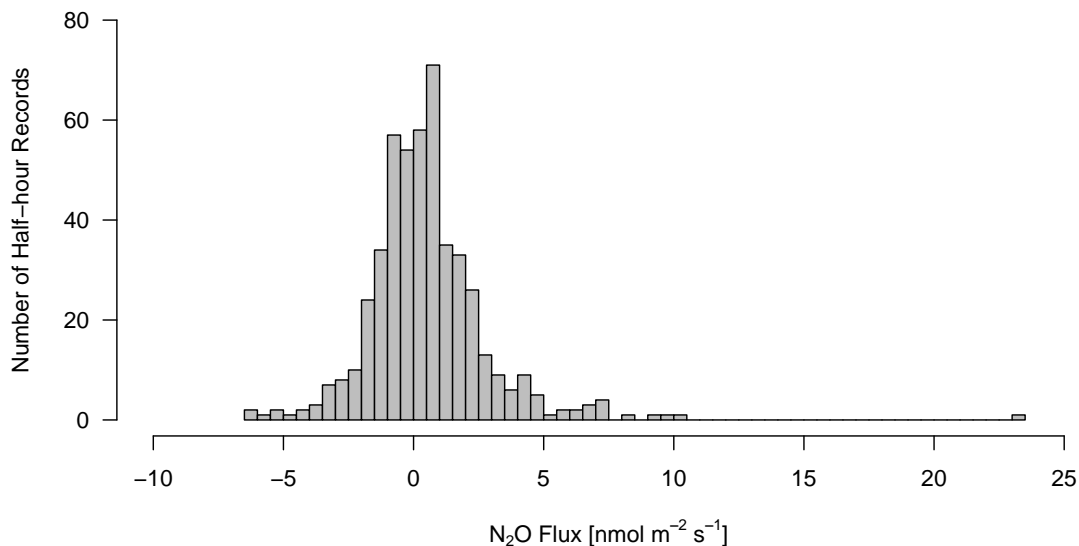
Fig. 5. Histogram of all significant N_2O fluxes after the density flux correction according to Webb et al. (1980). Only 44% of all available 30-min records (N=1107) were considered significant fluxes based on the significance-of-correlation criterion.
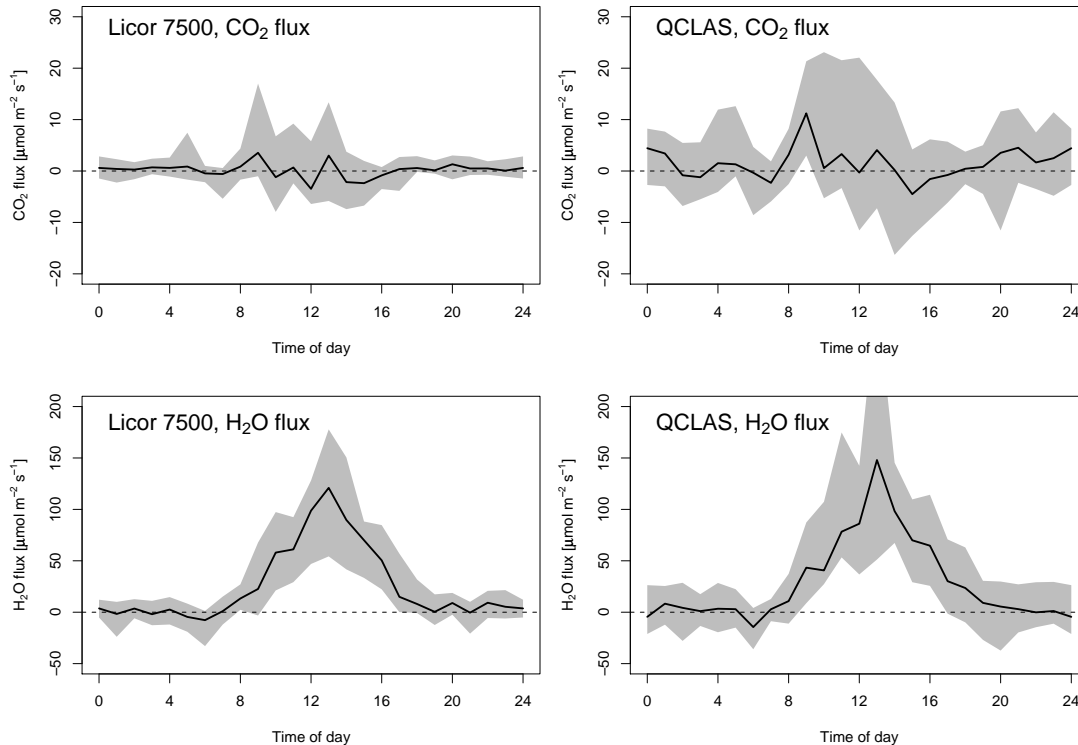
Fig. 6. Comparison of concurrent CO_2 (top) and H_2O (bottom) flux measurements obtained from an open-path IRGA (left; Licor 7500) and the closed-path QCLAS (right) using the same wind vector data. Bold lines and gray shaded areas show the median and interquartile range of the diurnal cycles. Data were lumped into 1-h bins for this comparison.

EGU
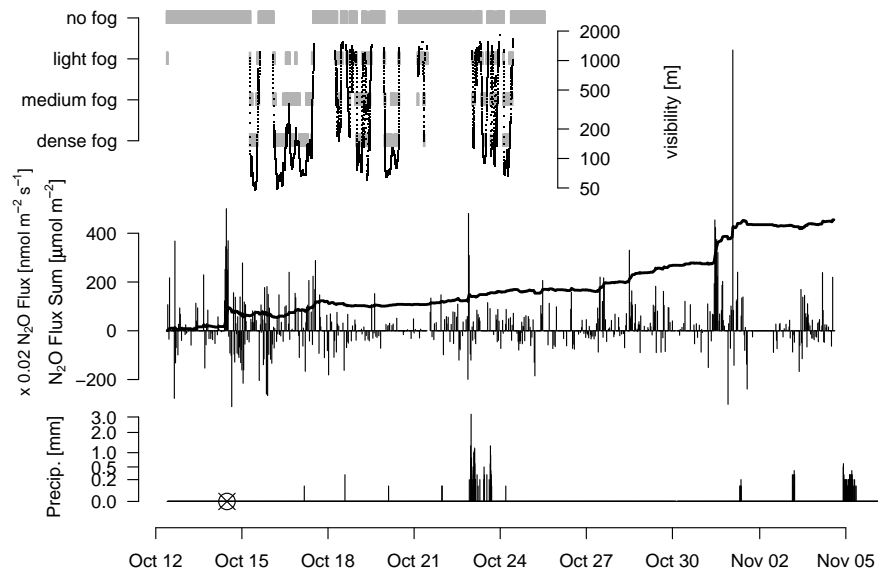
Fig. 7. N$_2$O fluxes during a 4-week period in autumn 2005 (middle panel; thin bars: 30-min averages; bold line: cumulative fluxes) measured over a beech-dominated mixed forest at the Lägeren, Switzerland, flux site. The top and bottom panels show the fog and rainfall conditions, respectively. Horizontal visibilities <1000 m are defined as fog (Glickman, 2000). The horizontal gray bars indicate the periods with no fog, light, medium, or dense fog. The crossed circle in the precipitation time series indicates a missing value that was generated by the plausibility check algorithm used by the data owners and indicates that although this precipitation value was screened out, this might have been a relevant event for N$_2$O fluxes.
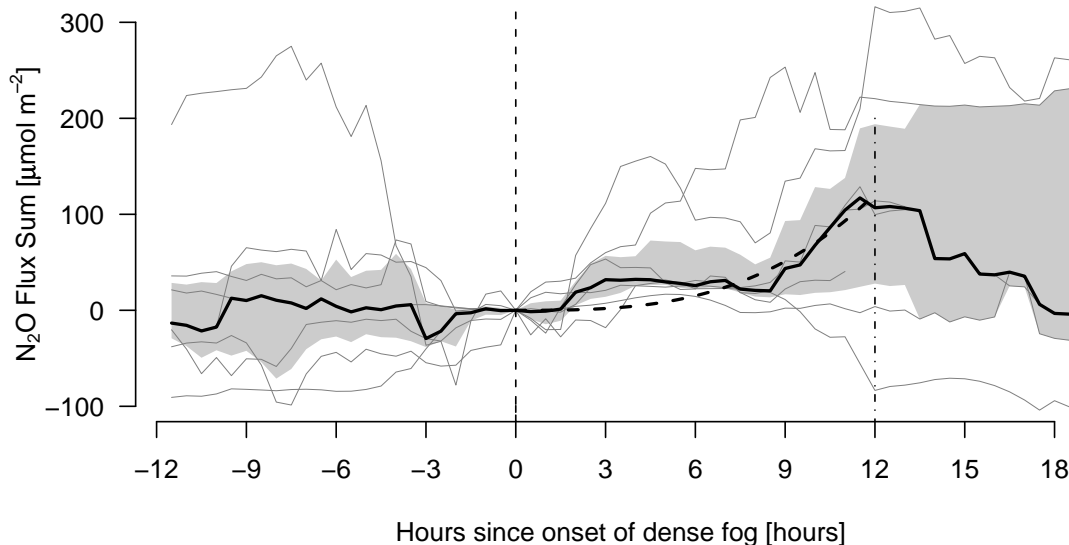
Fig. 8. Composite of N_2O flux sums during the 12 h before until 18 h after the onset of dense fog (threshold of 100 m horizontal visibility). Gray lines are shown for each of the 7 events. Bold line and gray-shaded area show the median and interquartile range, respectively. The thick broken line shows the tendency of the fluxes in the first 12 h after the onset of dense fog ($y = 0.07 \cdot t^3$ with t in hours since beginning of event). Events with <5 h duration were not included in this analysis.
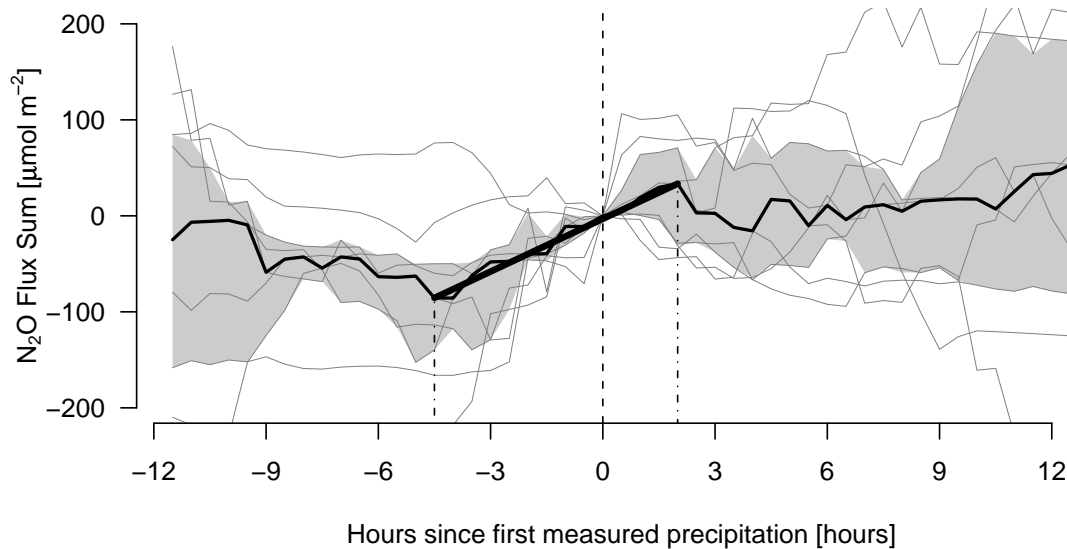
Fig. 9. Composite of N_2O flux sums during the 24-h period centered at the beginning of a precipitation event. Gray lines are shown for each of the 9 events. Bold line and gray-shaded area show the median and interquartile range, respectively. The regression line shows the best fit to the median conditions starting from 4.5 h before until 2 h after the onset of rainfall. See text for interpretation.